



Theoretical Analysis of Squeeze Lubrication Using Double ZZ Transform: Application of Non-Newtonian Fluids

Rehab Ali Khudair^{1*}, Enas Yahya Abdullah², Athraa Neamah Albukhuttar¹

¹ Department of Mathematics, Faculty of Education for Girls, Kufa University, Najaf 54002, Iraq

² Department of Mathematics, Faculty of Education, Kufa University, Najaf 54002, Iraq

Corresponding Author Email: rihaba.khudair@uokufa.edu.iq

Copyright: ©2024 The authors. This article is published by IETA and is licensed under the CC BY 4.0 license (<http://creativecommons.org/licenses/by/4.0/>).

<https://doi.org/10.18280/mmp.110401>

ABSTRACT

Received: 5 August 2023

Revised: 30 October 2023

Accepted: 10 November 2023

Available online: 26 April 2024

Keywords:

non-Newtonian fluids, mathematical model, double ZZ transform synovial joint, squeeze pressure

This paper highlights the flow of non-Newtonian fluids through porous elastic layers of human articular cartilage and describes the effect of lubricating fluid flow on the performance of daily activities and various activities with high accuracy through the design of a mathematical model. The current work includes the equations of motion, the equation of continuity, and squeeze lubrication as influencing factors on phases (stance phase-swing phase) in the gait cycle. In other words, study the characteristics of lubrication through the cohesive force of particles, initial concentration, smoothness of the surface, vertical roughness, and the weight of the human body. These expressions are computed using the double ZZ transformation and are used to describe many problems in the field of science, including the heat equation, Klein–Gordon equation, and others, all of which are crucial for physical applications and fractional differential equation because of its frequent appearance in fluid mechanics, mathematical biology, electrochemistry, and physics. The current findings show that solving these equations by Using single transforms is more difficult than using the double transform, because using a double transform the partial equation is converted directly into an algebraic equation, while the single transform converts the partial equation into an ordinary equation firstly and then into an algebraic equation, which requires more calculation and methods to obtain the exact solution. Besides, the theoretical and applied description of the lubrication mechanism is evident when hydrodynamic pressure is generated between the different layers, which plays an important role in the kinematic friction force between layers and particles. Furthermore, the results are presented graphically. From the analysis and computations of the results, it is found that the pressure and friction forces increase with an increase in the cycle of time. Cycle time greatly affects (pressure - friction force). It is known that the walking pattern varies depending on the daily activities that a person performs, which is greatly reflected in the increased pressure on the synovial joints, which is reflected in the increased friction between the (layer - molecules) responsible for lubricating articular.

1. INTRODUCTION

The idea of “integral transforms give us power and ease to solve such fundamental problems as initial value ones of a linear and of an integral differential equation, and numerous mathematicians across the world became interested in this problem during the last decades” of their applications of fluid mechanics was of great interest to the authors such as Sumudu, ARA, Saban, SEA, and SEJI [1-7].

Most problems in applied science and engineering fall under double integral equations or partial differential equations that are used to describe the nature and behavior of the physical outcome. Finally, the researcher concluded that, two years ago, 2016, Ranjit and Waghmare [8] hard work led to developing single transform to double transform partial equations that help in most mathematics problems to date. Ranjit and Waghmare 2016 applied the double Laplace double

transform method to get the linear/nonlinear space-time exact solutions of the time-fractional telegraph when they considered t double Laplace finds the solution. Conclusion Ranjit and Waghmare t double Laplace transform method reduces the computational work volume since it is easier in solving partial equations as compared to single Laplace because the solution to the problems does not require an A domain polynomial, Lagrange multiplier value, He’s polynomials, and small parameters.

Especially, compared to the numerical ones, the double Laplace transform has quite common use to solve the partial differential equations with unknown functions of two variables, which is general, and less easy to check in a numerical way. Therefore, it is highly advisable to check the performance of numerical methods to find the model error with analytical ones, which have developed and become more available. One of highly effective such analytical methods is

the integral transformations, which are used to find analytical solutions of partial differential equations. Apart from the discussed double Laplace transform, there are other applications in the literature as the double extensions of the double Laplace transform and double Shuhu and double ARA-Sumudu transforms [9-11].

In 2016, Zafar [12] introduced a new integral transform ‘ZZ Transform Method’ and it was used for the new integral transform technique application to solve first order linear differential equation, for example, Law of Natural Growth or Law of Natural Decay. ZZ transform Method is used for differential equation with variable coefficients. In 2022 a new transform, the double ZZ transform, was developed by researchers to extend the one-dimensional ZZ transform to two dimensions [13, 14]. We have also derived a few important theorems and properties. this method the Partial Differential equation is resolved without converting it to ordinary differential equation i.e., it is not necessary to determine the complete solution of Ordinary differential equation. This is the most important advantage of this method. Thus, it is very convenient & effective method. To demonstrate the effectiveness and great accuracy of the suggested transform, the transform is employed to find a solution to the popular squeeze action issue for unstable and incompressible fluid flow through the porous elastic of layers. By pressing the synovial fluid, the squeeze lubrication generates the hydrodynamic pressure. Both human articular mobility and synovial joints are required. The interstitial fluid must be removed from the solid organic matrix when the cartilages are squeezed under physiologically normal conditions (see Figure 1). The synovial fluid causes the interstitial fluid of the solid organic matrix to move relatively and to get drained by convection and diffusion [15, 16]. The amount of hyaluronic acid in the synovial fluid rises with lubrication and therefore imbibition and excretion of the solid mass increases its concentration [17, 18]. As cited by Wegamir increasing the concentration of Hyaluronic acid increases the viscosity of synovial fluid.

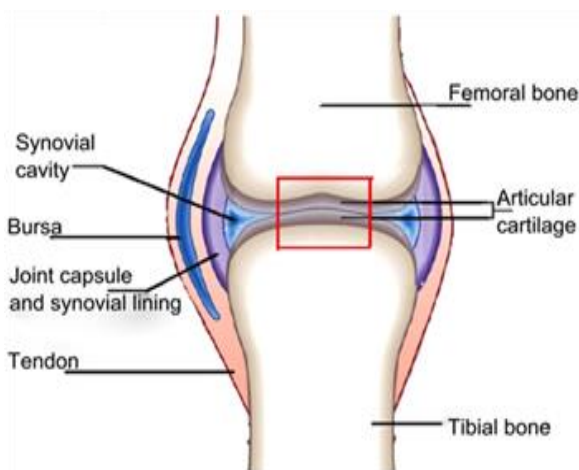


Figure 1. Physical information of synovial joint (Human knee joint) [19]

Squeeze lubrication occurs when the bearing surfaces move at right angles to each other. The pressure in the fluid film is generated by the movement of the articular surfaces parallel to each other. As the approaching surfaces come closer, the competing surfaces force the air out of the area of contact. The

pressure is caused by the attraction force that exists between the surfaces in the field of the lubricant, which persists as the fluid film is compressed. The squeeze lubrication is useful in short, high-pressure utilization. The demand of this device comes from a frequent pressure generation [20].

The pressure yielded in the femur-humerus and between the head of the femur and the tibia on the intervention of the synovial fluid is an example. It is significant because it is more directly related to the gait phase while it can only sustain twice the weight of the individual due to movement. The lubricating fluid is flowing through the pores of the articular cartilage to the lubricated when the movements are taking place. The amount of fluid remains constant, but the pressure emerged from the action of one layer of fluid compressing one another varies centuries.

2. BASIC DEFINITION OF FRACTIONAL CALCULUS

In this section, the study provides some basic definitions and theories of the double ZZ transform that will be used in this article:

2.1 Definition [12]

Let $\varphi(t)$ be a function defined for all $t \geq 0$, then ZZ transform of $\varphi(t)$ is the function $Z(\gamma, \rho)$ is defined by:

$$Z(\gamma, \rho) = \beta\{\varphi(t)\} = \frac{\rho}{\gamma} \int_0^{\infty} \varphi(t) e^{-\frac{\rho}{\gamma}t} dt \quad (1)$$

The inverse ZZ-transform of $Z(\gamma, \rho)$ and it is defined as $\beta\{\varphi(t)\} = Z^{-1}(Z(\gamma, \rho))$, where Z^{-1} is the inverse ZZ-transform operator.

2.2 Definition [13]

The double ZZ transform of the function $\varphi(x, t)$ is defined by the double integral as:

$$\beta^2\{\varphi(x, t)\} = Z((\theta, \rho), (\omega, \gamma)) = \frac{\theta}{\omega} \frac{\rho}{\gamma} \int_0^{\infty} \int_0^{\infty} \varphi(x, t) e^{-\left(\frac{\theta}{\omega}x + \frac{\rho}{\gamma}t\right)} dx dt \quad (2)$$

The inverse double ZZ-transform of $Z((\theta, \rho), (\omega, \gamma))$ and it is defined as $\beta^2\{\varphi(x, t)\} = Z^{-1}(Z((\theta, \rho), (\omega, \gamma)))$, where Z^{-1} is the inverse ZZ-transform operator.

Table 1 shows double ZZ transform for some special functions [13].

Table 1. Double ZZ transform for some special functions [13]

$\varphi(x, t)$	$\beta^2\{\varphi(x, t)\}$	$\varphi(x, t)$	$\beta^2\{\varphi(x, t)\}$
k	k	$\cos(ax+\epsilon t)$	$\frac{\theta\rho(\theta\rho - \alpha\epsilon\gamma\omega)}{(\theta^2 + \alpha^2\omega^2)(\rho^2 + \epsilon^2\gamma^2)}$
$e^{(\alpha x + \epsilon t)}$	$\frac{\theta\rho}{(\theta - \alpha\omega)(\rho - \epsilon\gamma)}$	$\sin(ax+\epsilon t)$	$\frac{\theta\rho(\epsilon\theta\gamma + \alpha\omega\rho)}{(\theta^2 + \alpha^2\omega^2)(\rho^2 + \epsilon^2\gamma^2)}$
$x^\delta y^\epsilon$	$\delta! \epsilon! \left(\frac{\omega}{\theta}\right)^\delta \left(\frac{\gamma}{\rho}\right)^\epsilon$	$\cosh(\alpha+\epsilon t)$	$\frac{\theta\rho(\theta\rho + \alpha\epsilon\gamma\omega)}{(\theta^2 - \alpha^2\omega^2)(\rho^2 - \epsilon^2\gamma^2)}$

2.3 Theorem [13]

Double ZZ transform of first and second order partial

derivatives are in the form:

$$\begin{aligned} \beta^2 \left\{ \frac{\partial \varphi(x, t)}{\partial x} \right\} &= \frac{\theta}{\omega} (Z(\theta, \rho) - \beta(\varphi(0, t))) \\ \beta^2 \left\{ \frac{\partial^2 \varphi(x, t)}{\partial x^2} \right\} &= \frac{\theta^2}{\omega^2} (Z((\theta, \rho), (\omega, \gamma)) - \beta(\varphi(0, t))) \\ &\quad - \frac{\theta}{\omega} \left(\frac{\partial}{\partial x} \beta(\varphi(0, t)) \right) \\ \beta^2 \left\{ \frac{\partial \varphi(x, t)}{\partial t} \right\} &= \frac{\rho}{\gamma} (Z((\theta, \rho), (\omega, \gamma)) - \beta(\varphi(x, 0))) \\ \beta^2 \left\{ \frac{\partial^2 \varphi(x, t)}{\partial t^2} \right\} &= \frac{\rho^2}{\gamma^2} (Z((\theta, \rho), (\omega, \gamma)) - \beta(\varphi(x, 0))) \\ &\quad - \frac{\rho}{\gamma} \left(\frac{\partial}{\partial t} \beta(\varphi(x, 0)) \right) \\ \beta^2 \left\{ \frac{\partial^2 \varphi(x, t)}{\partial x \partial t} \right\} &= \frac{\theta}{\omega} \varphi(0, 0) - \frac{\theta}{\omega} \beta(\varphi(0, t)) \\ &\quad + \frac{\theta}{\omega} \left(\frac{\rho}{\gamma} (Z((\theta, \rho), (\omega, \gamma)) - \beta(\varphi(x, 0))) \right) \end{aligned}$$

3. ASSUMPTIONS OF SQUEEZE LUBRICATION

Some of assumptions have been adopted in the current study:

- (1) Non-Newtonian fluid
- (2) Incompressible squeeze lubrication fluid
- (3) Unsteady
- (4) Neglect bodily forces like gravity and magnetic field
- (5) In fluid dynamics, the no-slip condition for viscous fluids assumes that at a solid boundary, the fluid will have zero velocity relative to the boundary. The fluid velocity at all fluid–solid boundaries is equal to that of the solid boundary.

4. DATA REDUCTION

4.1 Basic equation

The main equations that describe the theoretical analysis of the characteristics of the squeeze pressure region of the synovial fluid for the human joint can be derived and be a function of the phases of movement and gait of the synovial joint and the mathematical model and result analysis of the squeeze lubrication when the above-mentioned boundary conditions are addressed. This is a deterministic analysis and the effects of squeeze lubrication and the pressure and the friction force between the synovial fluid particles and the synovial fluid particles and layers against themselves are considered simultaneously.

4.2 Mathematical formulation of the problem

The continuity equation simply expresses the law of conservation of mass (mass per unit time entering the tube must flow out at same rate). The equation of continuity in cylindrical coordinates when the fluid is non-compressible, is written as follows:

$$\frac{u}{r} + \frac{\partial u}{\partial r} + \frac{1}{r} \frac{\partial v}{\partial \theta} + \frac{\partial w}{\partial z} = 0$$

The equations of motion of a real fluid can be developed from consideration of the force action on a small element of

the fluid including the shear stresses generated by fluid motion and viscosity. These equations are called Navier- Stokes is written as follows:

$$\frac{Du}{Dt} - \frac{v^2}{r} = F_r - \frac{1}{\rho} \frac{\partial p}{\partial r} + v(\nabla^2 u - \frac{u}{r^2} - \frac{2}{r^2} \frac{\partial u}{\partial \theta})$$

After applying the assumptions of squeeze lubrication, the equations responsible the flow with (turbulent – regular) through porous elastic layers become follows:

$$\frac{\partial^2 u}{\partial z^2} = \frac{1}{\mu} \frac{\partial p}{\partial r} (1 + L + w + v) \quad (3)$$

$$\frac{\partial^2 v}{\partial z^2} = S_r \quad (4)$$

$$\frac{\partial u}{\partial r} + \frac{\partial w}{\partial z} = 0 \quad (5)$$

With nondimensional initial and boundary conditions:

$$\begin{aligned} v(r, 0) &= C_0, v_z(r, 0) = C_1, u(r, h) = \frac{\partial h}{\partial t} U_1, \\ u(r, -h) &= \frac{\partial h}{\partial t} U_2, w(r, z) = 0, w(r, z) = h \frac{\partial^2 h}{\partial r \partial t} \end{aligned} \quad (6)$$

where, $S_r = \frac{D_n K_T (T_1 - T_0)}{r_n (C_1 - C_0)}$, $w = \frac{S_p}{R cent}$. Where r body force, (u , w) are the velocity components of the lubricant in r and directions respectively, P is pressure, μ dynamic viscosity, L stride length, w is weight of human and S_r sote's number.

By taking double ZZ transform to Eq. (4) and using boundary condition of the tangential component of the fluid velocity in the film region:

$$v(r, 0) = C_0, v_z(r, 0) = C_1 \quad (7)$$

where,

$$\begin{aligned} G(x, 0) &= C_0, \frac{\partial}{\partial z} G(x, 0) = C_1 \\ \frac{\rho^2}{\gamma^2} \left(G((\theta, \rho), (\omega, \gamma)) - G(x, 0) \right) - \frac{\rho}{\gamma} \left(\frac{\partial}{\partial z} G(x, 0) \right) &= \frac{1}{\mu} \end{aligned} \quad (8)$$

$$v(x, z) = \frac{1}{2} S_r z^2 + C_1 z + C_0 \quad (9)$$

Now, modifying the film region Eq. (3) of the Navier-Stokes equation to include the tangential component of fluid velocity:

$$\begin{aligned} \frac{\partial^2 u}{\partial z^2} &= \frac{1}{\mu} \frac{\partial p}{\partial r} [1 + SL + w + v] = \frac{1}{\mu} \frac{\partial p}{\partial r} \\ &\quad \left[1 + Sl + w + \frac{1}{2} S_r z^2 + C_1 z \right] + C_0 \end{aligned} \quad (10)$$

Then:

$$\begin{aligned} \frac{\rho^2}{\gamma^2} \left(G((\theta, \rho), (\omega, \gamma)) - G(x, 0) \right) - \frac{\rho}{\gamma} \left(\frac{\partial}{\partial z} G(x, 0) \right) \\ = \frac{1}{\mu} \frac{\partial p}{\partial r} \left[(1 + Sl + w + C_0) + \frac{1}{2} S_r \frac{\gamma^2}{\rho^2} + C_1 \frac{\gamma}{\rho} \right] \end{aligned} \quad (11)$$

$$u(r, z) = \frac{1}{\mu} \frac{\partial p}{\partial r} \left[(1 + Sl + w + C_0) \frac{z^2}{2} + \frac{1}{24} S_r z^4 + C_1 z^3 \right] + A_1 z + B_1 \quad (12)$$

After substitution a boundary condition $u(r, h) = \frac{\partial h}{\partial t} U_1, u(r, -h) = \frac{\partial h}{\partial t} U_2$ and performing simple mathematical operations:

$$u(r, z) = \frac{1}{\mu} \frac{\partial p}{\partial r} \left[\frac{1}{2} (1 + Sl + w + C_0) (z^2 - h^2) - \frac{1}{24} S_r (z^4 - h^4) + \frac{1}{6} C_1 (z^3 - h^2 z) \right] + \frac{1}{2h} \frac{\partial h}{\partial t} (U_1 - U_2) z + \frac{1}{2} \frac{\partial h}{\partial t} (U_1 + U_2) \quad (13)$$

Integrating Eq. (5) with respect to z with the boundary conditions of $w(r, z) = 0, w(r, z) = h \frac{\partial^2 h}{\partial r \partial t}$, we can achieve the porosity non-Newtonian:

$$w(r, h) = \frac{\partial}{\partial r} \frac{1}{\mu} \frac{\partial p}{\partial r} \left(\frac{-1}{2} (1 + Sl + w + C_0) \left(\frac{1}{3} z^3 - h^2 z \right) - \frac{1}{24} S_r \left(\frac{1}{5} z^5 - h^4 z \right) - \frac{1}{6} C_1 \left(\frac{1}{4} z^4 - \frac{1}{2} h^2 z^2 \right) \right) - \frac{1}{2h} \frac{\partial h}{\partial t} (U_1 - U_2) \frac{z^2}{2} + \frac{1}{2} \frac{\partial h}{\partial t} (U_1 + U_2) z \quad (14)$$

$$h \frac{\partial^2 h}{\partial r \partial t} = - \frac{\partial^2 p}{\partial r^2} \left[\frac{1}{2} (1 + Sl + w + C_0) \left(\frac{1}{3} h^3 - h^3 \right) + \frac{1}{24} S_r \left(\frac{1}{5} h^5 - h^5 \right) + \frac{1}{6} C_1 \left(\frac{1}{4} h^4 - \frac{1}{2} h^4 \right) \right] - \frac{h}{4} \frac{\partial^2 h}{\partial r \partial t} (U_1 - U_2) + \frac{1}{2} \frac{\partial^2 h}{\partial r \partial t} (U_1 + U_2) h \quad (15)$$

4.3 Squeeze film pressure

For theoretical and computational reasons, it is crucial to include the non-dimensional parameters in the pressure's governing equations. The different lubricating system parameters should be presented in non-dimensional form as well.

$$p^* = - \frac{ph_c^2}{\mu R \frac{\partial^2 h}{\partial r \partial t}}, h_c = \frac{h}{h_0}, L = \frac{-LwH}{N} \quad (16)$$

$$w = \frac{-\bar{w}NR}{SL}, \beta = \frac{h_0}{R}, \bar{U} = \frac{-U_2}{U_1}, r^* = \frac{r}{R}$$

where, S, W, D are the stride length, body weight of human and distance.

Then,

$$\frac{\partial^2 p^*}{\partial r^{*2}} = \frac{-(1+0.25(3+\bar{U}))}{\left(\frac{1}{3} R^3 \left(1 - \frac{LwH}{N} \frac{\bar{w}NR}{SL} + C_0 \right) + \frac{1}{3} \beta R h_c (0.1 \beta R h_0 + 0.125 C_1) \right)} \quad (17)$$

After that:

$$\frac{\partial^2}{\omega^2} \left(G((\theta, \rho), (\omega, \gamma)) - G(0, z) \right) - \frac{\theta}{\omega} \left(\frac{\partial}{\partial x} G(0, z) \right) = \frac{-(1+0.25(3+\bar{U}))}{\left(\frac{1}{3} R^3 \left(1 - \frac{LwH}{N} \frac{\bar{w}NR}{SL} + C_0 \right) + \frac{1}{3} \beta R h_c (0.1 \beta R h_0 + 0.125 C_1) \right)} \quad (18)$$

$$p^*(r, z) = \frac{-(1+0.25(3+\bar{U}))}{\left(\frac{1}{3} R^3 \left(1 - \frac{LwH}{N} \frac{\bar{w}NR}{SL} + C_0 \right) + \frac{1}{3} \beta R h_c (0.1 \beta R h_0 + 0.125 C_1) \right)} + A_2 r^* + B_2 \quad (19)$$

After substitution a boundary condition $p^*(1, z) = 0, \frac{\partial}{\partial x} p^*(0, z) = 0$ in Eq. (19) and performing simple mathematical operations, we get:

$$p^*(r, z) = \frac{1.5(1-r^{*2})(1+0.25(3+\bar{U}))}{\left(\frac{1}{3} R^3 \left(1 - \frac{LwH}{N} \frac{\bar{w}NR}{SL} + C_0 \right) + \frac{1}{3} \beta R h_c (0.1 \beta R h_0 + 0.125 C_1) \right)} \quad (20)$$

4.4 Friction force

The friction force between layers the particles of synovial fluid is very important factor. We will study set of internal factors that affect the force of friction, assume that non-Newtonian fluid and Newton low of viscosity be:

$$\tau = \mu \left(\frac{\partial u}{\partial z} \right) \quad (21)$$

where, μ is dynamic viscosity and the term $\left(\frac{\partial u}{\partial z} \right)$ velocity gradient of z is obtained from the velocity distribution.

$$\frac{\partial u}{\partial z} = \frac{1}{\mu} \frac{\partial p}{\partial x} R_a \bar{\mu} \left(\frac{h^2}{2} - z^2 \right) + \frac{Q \bar{u} t}{h^3} \quad (22)$$

$$\mu \frac{\partial u}{\partial z} = \frac{\partial p}{\partial x} R_a \bar{\mu} \left(\frac{h^2}{2} - z^2 \right) + \frac{\mu Q \bar{u} t}{h^3} \quad (23)$$

$$F = \int_0^R \mu \frac{\partial u}{\partial z} dr \quad (24)$$

where, $z=h$ (film thickness).

$$F_h = \int_0^R \left(\frac{\partial p}{\partial r} R_a \bar{\mu} \left(\frac{h^2}{2} - z^2 \right) + \frac{\mu Q \bar{u} t}{h^3} \right) dr \quad (25)$$

$$F_h = \int_0^R \left(\frac{\partial p}{\partial r} R_a \bar{\mu} \left(- \frac{h^2}{2} \right) + \frac{\mu Q \bar{u} t}{h^3} \right) dr \quad (26)$$

Now, we have been presented dimensionless friction force:

$$F^*_h = \frac{F_h}{\mu \bar{u} H_0}, r^* = \frac{r}{H_0}, p^* = \frac{p h^2}{\mu \bar{u} H_0} \quad (27)$$

After have been applied Eq. (21) in Eq. (20), then:

$$F^*_h = \int_0^{R^*} \left(- \frac{\partial p^*}{\partial r^*} \bar{\mu} \left(\frac{R_a}{2} \right) + Q^* \right) \partial r^* \quad (28)$$

$$p^*(r, z) = \frac{1.5(1-r^{*2})(1+0.25(3+\bar{U}))}{\left(\frac{1}{3} R^3 \left(1 - \frac{LwH}{N} \frac{\bar{w}NR}{SL} + C_0 \right) + \frac{1}{3} \beta R h_c (0.1 \beta R h_0 + 0.125 C_1) \right)}$$

Now, derivative the dimensionless squeeze film pressure (p^*) respect to r^* and substitute in Eq. (22):

$$F^*_h = \int_0^{r^*} \left(- \frac{1.5(1-r^{*2})(1+0.25(3+\bar{U}))}{\left(\frac{1}{3} R^3 \left(1 - \frac{LwH}{N} \frac{\bar{w}NR}{SL} + C_0 \right) + \frac{1}{3} \beta R h_c (0.1 \beta R h_0 + 0.125 C_1) \right)} \bar{\mu} \left(\frac{R_a}{2} \right) + Q^* \right) \partial r^* \quad (29)$$

$$F^*_h = - \frac{(0.75 R^{*2})(1+0.25(3+\bar{U}))(\bar{\mu} R_a)}{\left(\frac{1}{3} R^3 \left(1 - \frac{LwH}{N} \frac{\bar{w}NR}{SL} + C_0 \right) + \frac{1}{3} \beta R h_c (0.1 \beta R h_0 + 0.125 C_1) \right)}$$

5. RESULTS AND DISCUSSION

5.1 Squeeze pressure

The variation of the dimensionless squeeze film pressure (p^*) generated by the squeeze film action as a function of

dimensionless distance (r^*) for different values of fluid velocity (\vec{U}) is shown in Figure 2 and Table 2 with using Eq. (20). It is observed increase in the velocity of the synovial fluid particles leads to the movement of the particles, which leads to an increase in the rate of collision of the particles and the viscosity of the synovial fluid increases, and thus the pressure increases.

Table 2. Relationship between velocity of particles and pressure

After 20-Cycle Time					
Velocity	0.1	0.5	1	1.5	1.9
Pressure	2.14439	2.2652	2.41621	2.56722	2.68803
After 80-Cycle Time					
Velocity	2	2.5	3	3.5	3.9
Pressure	2.71824	2.86925	3.02026	3.17127	3.29909
After 250-Cycle Time					
Velocity	4	4.5	5	5.5	6
Pressure	3.32229	3.4733	3.62431	3.77533	3.92634

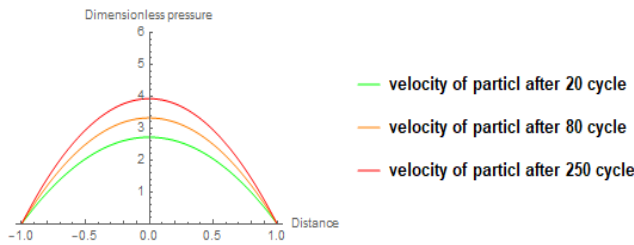


Figure 2. Variation of dimensionless pressure (p^*) for different parametric of velocity parameters (\vec{U})

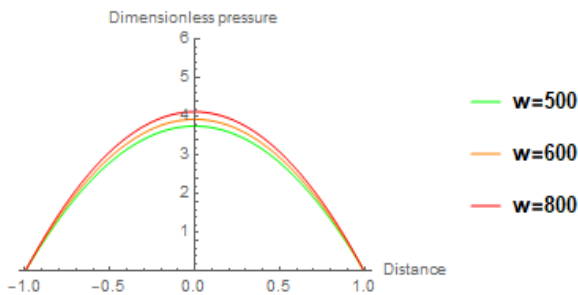


Figure 3. Variation of dimensionless pressure (p^*) for different parametric of weight of human parameters (w)

The different dimensionless pressure distribution for different value weight of human is seen in Figure 3 and Table 3. It is found that the pressure increases with the increase in weight of the human and time of cycle, and the explanation is that the longer the cycle, which leads to an increase in the rate of flow of lubricant from the porosity and with the different activities performed by the person, the weight doubles and the production of lubricants decreases.

The variation of the dimensionless squeeze film pressure (p^*) generated by the squeeze film action as a function of dimensionless distance (r^*) for different values of fluid concentration (C_0) is seen in Figure 4 and Table 4. It is cleared the dimensionless pressure increasing and become more with decreasing value of synovial fluid concentration ($C_0=0.2$) inversely, increasing fluid initial concentration ($C_0=0.6$) that lead to decreasing in dimensionless pressure.

Table 3. Relationship between weight of human and pressure

After 20-Cycle Time					
Weight of human	50	60	70	80	90
Pressure	2.59715	2.71921	2.85332	3.00133	3.16554
After 80-Cycle Time					
Weight of human	50	60	70	80	90
Pressure	3.1743	3.32348	3.48739	3.66829	3.869
After 250-Cycle Time					
Weight of human	50	60	70	80	90
Pressure	3.75144	3.92776	4.12146	4.33526	4.57245

Table 4. Relationship between initial constriction and pressure

After 20-Cycle Time					
Cohesion strength	3	4	5	6	7
Pressure	3.76806	3.15663	2.87804	2.71792	2.61697
After 80-Cycle Time					
Cohesion strength	3	4	5	6	7
Pressure	4.60541	3.8581	3.5176	3.32348	3.19851
After 250-Cycle Time					
Cohesion strength	3	4	5	6	7
Pressure	5.4427	4.55957	4.15717	3.92775	3.78006

The relationship between dimensionless hydrodynamic pressure (p^*) with different porosity of articular cartilage (β) is shown in Figure 5. As a result, it can be seen that reducing the porosity causes additional outflow of synovial fluid from synovial cells, which, in turn, increases the hydrodynamic pressure between layers. At the brushes in non-Newtonian lubrication for film thickness involves the cycle time becomes a minimum film thickness, and again, time is necessary. The effect of a film thickness parameter (H) of gab between two articulates on the variation (p^*) is demonstrated in Figure 6.

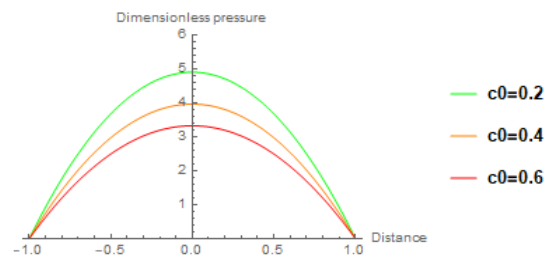


Figure 4. Variation of dimensionless pressure (p^*) for different parametric of initial concentration (c_0)

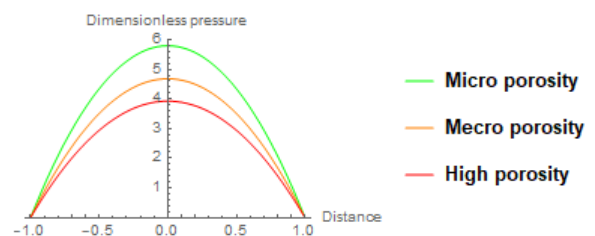


Figure 5. The variation of dimensionless pressure (p^*) for different parametric porosity parameters (β)

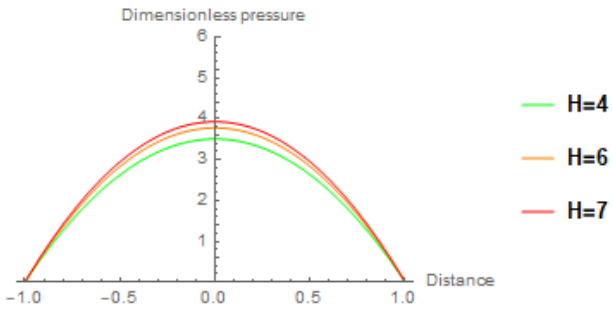


Figure 6. Variation of dimensionless pressure (p^*) for different parametric of film thickness (H)

It is observed increases values of (h^*), when flexibility of synovial joint to lead increase pressure (p^*) because the expand the tissue and thus increasing the flow of fluid responsible for generating pressure and effective radius of curvature parameter (R) on the variations of (p^*) is shown in Figure 7. It is observed that the pressure film (p^*) increases with the decreasing value of (R).

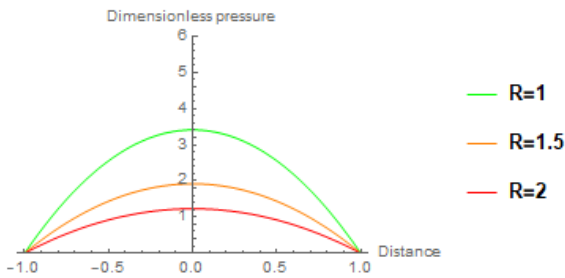


Figure 7. Variation of dimensionless pressure (p^*) for different parametric curvature parameter (R)



Figure 8. Variation of dimensionless Kinematic friction force (ζ^*) with gait phase (ω) for different parametric of viscosity parameters ($\bar{\mu}$)

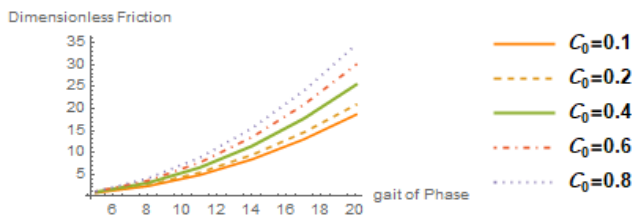


Figure 9. Variation of dimensionless Kinematic friction force (ζ^*) with gait phase (ω) for different initial concentration

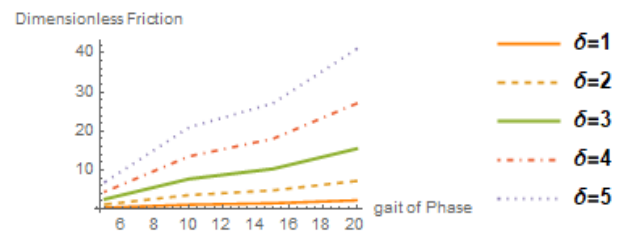
5.2 Kinematic friction force

Kinetic friction force is the force that occurs when resisting

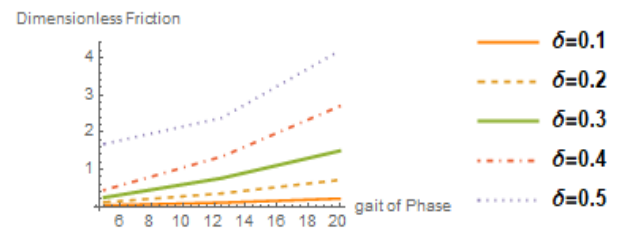
motion due to contact between a layer and a particle that is moving against it. The current study has dealt with a set of internal factors that affect the force of friction and after applying Eq. (29) to these factors using a 12 mathematical program. Dimensional friction force (ζ^*) as a function of the gait phase (ω) for different values of different viscosity ($\bar{\mu}$), high viscosity means an increase in the cohesion force between the molecules, which leads to a high kinetic friction force between molecules. The friction force is related to the phases of movement in a direct relationship as shown in the Table 5 and Figure 8. Dimensional friction force (ζ^*) as a function of the gait phase (ω) for different initial concentration (c_0). The force of adhesion between particles when it is high, the concentration of the liquid is high, especially in the phase of heel contact as shown Figure 9.

Table 5. Relationship between parametric of viscosity parameters ($\bar{\mu}$) and Kinematic friction force (ζ^*)

Parametric of Viscosity	$\omega=5$	$\omega=10$	$\omega=15$	$\omega=20$	$\omega=25$
Parameters ($\bar{\mu}$)	ζ^*	ζ^*	ζ^*	ζ^*	ζ^*
0.01	0.37	1.20	2.57	4.50	6.98
0.02	0.65	2.30	5.05	8.91	13.87
0.03	0.92	3.40	7.53	13.39	20.75



(a)



(b)

Figure 10. Variation of dimensionless Kinematic friction force (ζ^*) with gait phase (ω) for different the nature of the contacting surfaces: (a) surface roughness; (b) surface smooth

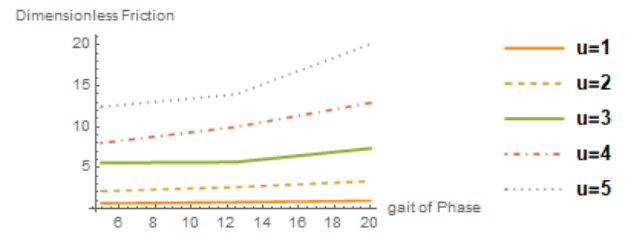
Table 6. Relationship between parametric of the nature of the contacting surfaces: (a) surface roughness; (b) surface smooth (ζ) and Kinematic friction force (ζ^*)

	Surface Roughness			Surface Smooth		
	Loading response					
ζ	1	3	6	0.1	0.3	0.6
ζ^*	0.37	1.50	2.25	0.037	0.112	0.22
	Early mid stance					
ζ	1	3	6	0.1	0.3	0.6
ζ^*	2.57	7.73	15.47	0.45	1.35	2.70
	ζ					
ζ	1	3	3	0.1	0.3	0.6
ζ^*	6.98	15.95	22.04	1.69	2.39	4.19

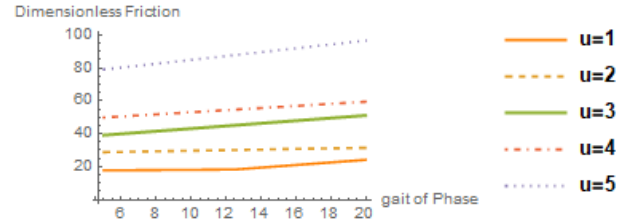
Dimensional friction force (ζ^*) as a function of the gait phase (ω) for different nature of the contacting surfaces (δ), the nature of the surface: Friction depends on the nature of the contacting surfaces, as rough surfaces will need more force to move them than if those surfaces are smooth, as the force of friction decreases with the increase in the smoothness of the body to a certain degree, but if it exceeds that degree, the friction actually increases between two surfaces They are very smooth due to the increased electrostatic forces between their molecules as shown in the Table 6 and Figure 10.

Dimensional friction force (ζ^*) as a function of the gait phase (ω) for regular velocity (\bar{u}). The lubricated liquid contains particles. The cohesion force between the particles increases with the increase in the flow velocity between the layers (superficial zone-middle zone-deep zone) and the walking stages, resulting in a high friction force of up to 80%.as shown in Figures 11 and 12. The lubricated fluid contains particles that have a high percentage of viscosity depending on the pattern of movement. The flow of the fluid loaded with particles increases as the speed increases. The friction between the particles increases with it. The rate of friction is higher in (superficial zone).

The force of friction does not depend on the area of contacting surfaces in moving objects, or on the relative velocity of those objects, but rather on the interconnecting forces arising between them, as shown in Figure 13. The force of friction is closely related to the phase of movement. In the phase (loading response), the flow of fluid increases through the porosity of the cartilage, which generates pressure between the layers that reduces friction. In the phase (early mid stance), the weight doubles and the flow of lubricants decreases, which makes the force of friction between the layers higher. In the phase (terminal), it increases in strength. Friction greatly affects the performance of the joint, and to reduce damage, we raise the fitness parameters, which are the focus of our study.



(a)



(b)

Figure 11. Variation of dimensionless Kinematic friction force (ζ^*) with gait phase (ω) for different velocity: (a) ($\omega=5-23$); ($\omega=35-55$)

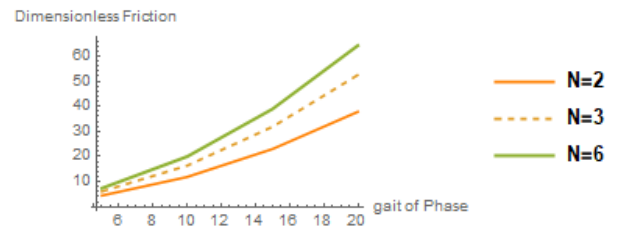


Figure 12. Variation of dimensionless Kinematic friction force (ζ^*) with gait phase (ω) for different cohesive force of particle

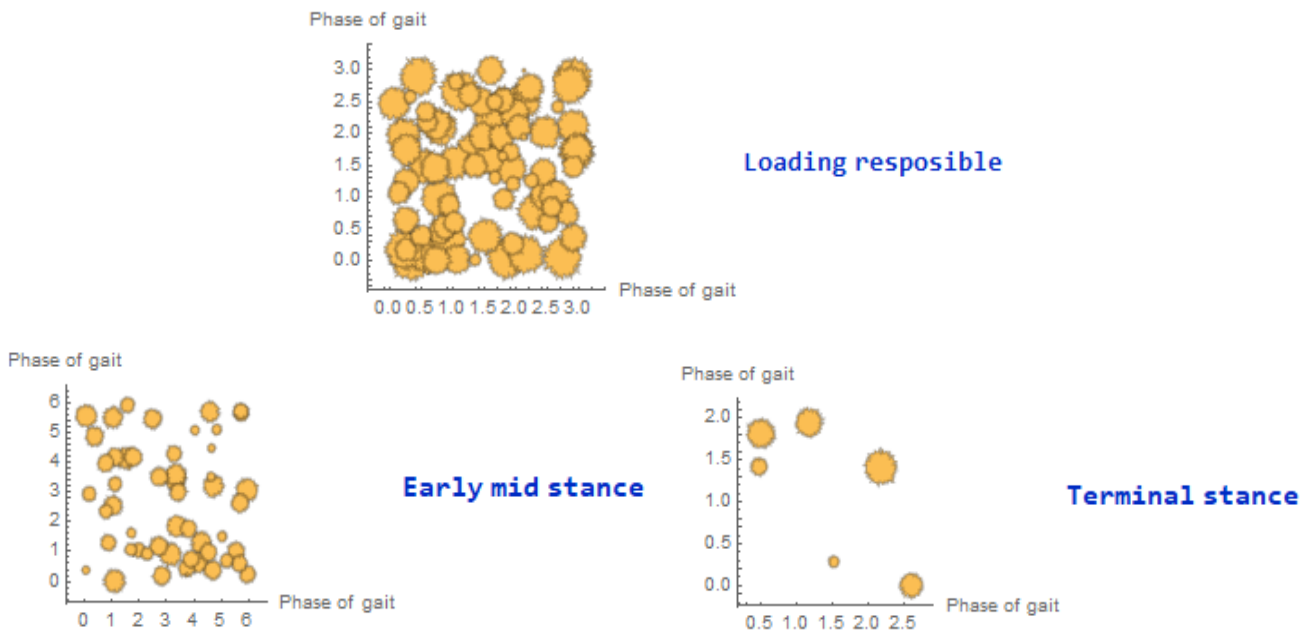


Figure 13. Relationship between Kinematic friction force (ζ^*) with gait phase (ω) (heel contact - loading response- early mid stance- terminal stance)

Dimensional friction force (ζ^*) as a function of the gait phase (ω) for regular velocity (β). Layer (superficial zone) is the most susceptible to kinetic friction due to the porosity size

of the penetration of particles and a decrease in the thickness of the cartilage layers, which greatly affects the friction force, as shown in Figures 14 and 15.

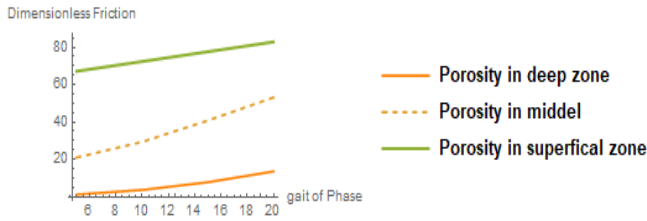


Figure 14. Variation of dimensionless Kinematic friction force (ζ^*) with gait phase (ω) for different porosity of layers

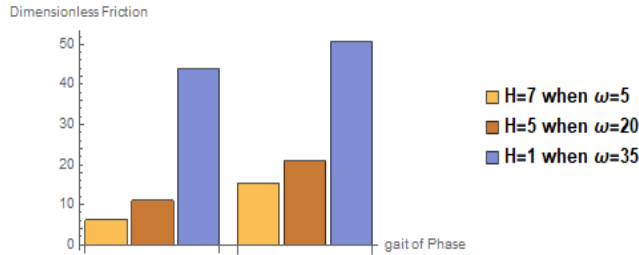


Figure 15. Variation of dimensionless Kinematic friction force (ζ^*) with gait phase (ω) for different film thickness

Dimensional friction force (ζ^*) as a function of the gait phase (ω) for weight of human (W). Body weight: An object moving over a horizontal surface exerts a force downward on that surface, as this force is equal to the weight of the body, as shown in Figure 16.

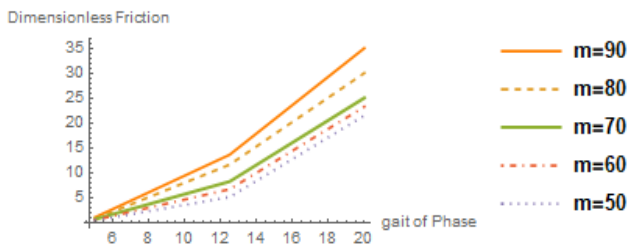


Figure 16. Variation of dimensionless Kinematic friction force (ζ^*) with gait phase (ω) for different weight of human

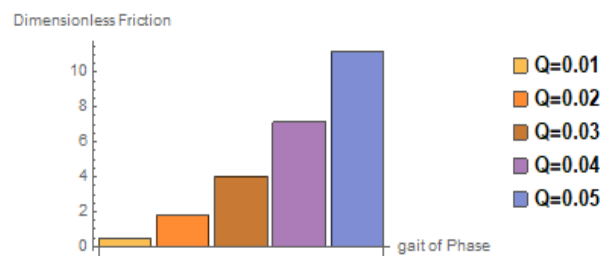


Figure 17. Variation of dimensionless Kinematic friction force (ζ^*) with gait phase (ω) for different flow force

Dimensional friction force (ζ^*) as a function of the gait phase (ω) for Kinematic friction force. The relationship between the kinetic friction force and the fluid flow force is a direct relationship, the greater the value of the fluid flow force, the greater the kinetic friction force, and the greater the body's resistance to movement, as shown in Figure 17.

6. CONCLUSIONS

In this paper, we investigate the flow of non-Newtonian fluids through the porous elastic layers of human articular cartilage and describe the impact of lubricating fluid flow on performance. In this research, we highlight (squeeze lubrication) the lubricated liquid and identify the most important parameters that affect the flow of the liquid and which are reflected in the movement mechanism, which represents an important element for performing daily activities. To accomplish these goals, the characteristics of lubrication through the cohesive force of particles, initial concentration, surface smoothness, vertical roughness, and human body weight are studied. These expressions are computed using the double ZZ transformation and are employed to describe numerous scientific problems. The current findings indicate that using single transforms to solve these equations is more difficult than using the double transform. In addition, both the theory and practise of lubrication are evident when hydrodynamic pressure is generated between distinct layers. This pressure contributes significantly to the kinematic force of friction between strata and particles. Kinetic friction between the layers is greatly affected by pressure, as high pressure generates high stress peaks that protect the layers and provide safety for the cartilage, and the opposite happens when pressure decreases. According to the analysis and computation of the results, the pressure and friction forces increase as the cycle time increases. Dynamic friction and pressure play a major role in the stages of walking. When the activities are recording, the applied pressure is increased. It is appropriate to learn the patterns of movement to reduce the harm, and the developed laws must define what combination of parameters influences on directions. It is possible to create doubles of ZZ applications and resolve coupled the differential equations and systems and PDEs with variable coefficients. The mentioned new double transform presents additional novelties comparable with the existing alternative methods as follows: The numerous advantages of our double ZZ sequence are that it can be used with a numerical iterative solution of nonlinear problems of PDEs.

REFERENCES

- [1] Belgacem, T.M., Arabli, A.A. (2006). Sumudu transform fundamental properties investigations and applications. *Journal of Applied Mathematics and Stochastic Analysis*, 2006: 91083. <https://doi.org/10.1155/JAMSA/2006/91083>
- [2] Saadeh, R., Qazza, A., Burqan, A. (2020). A new integral transform: ARA transform and its properties and applications. *Symmetry*, 12(6): 925. <https://doi.org/10.3390/sym12060925>
- [3] Khudair, R.A., Albukhuttar, A.N., Alkiffai, A.N. (2021). The new transform 'Shaban Transform' and its applications. *Smart Science*, 9(2): 103-112. <https://doi.org/10.1080/23080477.2021.1898796>
- [4] Shaban, R.A., Baqir, N.M. (2021). Using Shaban transformation for solving equations of the deflection curve. *Journal of Interdisciplinary Mathematics*, 24(7): 1771-1778. <https://doi.org/10.1080/09720502.2021.1960709>
- [5] Ali, A.H., Kuffi, E.A. (2022). The SEA transform and its

- application on differential equation. *International Journal of Health Sciences*, 6(S3): 613-622. <https://doi.org/10.53730/ijhs.v6nS3.5393>
- [6] Mehdi, S.A., Kuffi, E.A., Jasim, J.A. (2023). Solving the partial differential equations by using SEJI integral transform. *Journal of Interdisciplinary Mathematics*, 26(6): 1123-1132. <https://doi.org/10.47974/JIM-1611>
- [7] Mehdi, S.A., Kuffi, E.A., Jasim, J.A. (2023). SEJI integral transform of Bessel's functions. *Journal of Interdisciplinary Mathematics*, 26(6): 1159-1169. <https://doi.org/10.47974/JIM-1614>
- [8] Ranjit, R.D., Waghmare, G.L. (2016). Double Laplace transform method for solving space and time fractional telegraph equations. *International Journal of Mathematics and Mathematical Sciences*, 2016: 1414595. <https://doi.org/10.1155/2016/1414595>
- [9] Debnath, L. (2016). The double Laplace transforms and their properties with applications to functional, integral and partial differential equations. *International Journal of Applied and Computational Mathematics*, 2: 223-241. <https://doi.org/10.1007/s40819-015-0057-3>
- [10] Alfaqeh, S., Misirli, E. (2020). On double Shehu transform and its properties with applications. *International Journal of Analysis and Applications*, 18(3): 381-395. <https://doi.org/10.28924/2291-8639-18-2020-381>
- [11] Qazza, A., Burqan, A., Saadeh, R., Khalil, R. (2022). Applications on double ARA–Sumudu transform in solving fractional partial differential equations. *Symmetry*, 14(9): 1817. <https://doi.org/10.3390/sym14091817>
- [12] Zafar, Z.U.A. (2016). ZZ Transform Method. *International journal of advanced engineering and global technology*, 4: 1605-1611.
- [13] Shaban, R.A., Abdullah, E.Y., Albukhuttar, A.N. (2022). Study unsteady flow of synovial fluid in the elastic porosity of layers using double ZZ transformation. *Journal of Interdisciplinary Mathematics*, 25(6): 1933-1950. <https://doi.org/10.1080/09720502.2022.2093438>
- [14] Rao, R.U. (2017). ZZ transform method for natural growth and decay problems. *International Journal of Progressive Sciences and Technologies (IJPSAT)*, 5(2): 147-150.
- [15] Bali, R., Shukla, A.K. (2001). Rheological effects of synovial fluid on nutritional transport. *Tribology Letters*, 9: 233-239. <https://doi.org/10.1023/A:1018825425258>
- [16] Volkov, A.V., Novochadov, V.V. (2014). Crucial processes' interaction during the renewal of articular cartilage: The mathematical modeling. *European Journal of Molecular Biotechnology*, 4(2). <https://doi.org/10.13187/ejmb.2014.4.86>
- [17] Taylor, G.I. (1953). Dispersion of soluble matter in solvent flowing slowly through a tube. *Proceedings of the Royal Society of London. Series A. Mathematical and Physical Sciences*, 219(1137): 186-203. <https://doi.org/10.1098/rspa.1953.0139>
- [18] Aris, R. (1956). On the dispersion of solute in a fluid flow through a tube. *Proceedings of the Royal Society A*, 235. <https://doi.org/10.1098/rspa.1956.0065>
- [19] Tandon, P.N., Chaurasia, A., Jain, V.K., Gupta, T. (1991). Application of magnetic fields to synovial joints. *Computers & Mathematics with Applications*, 22(12): 33-45. [https://doi.org/10.1016/0898-1221\(91\)90145-T](https://doi.org/10.1016/0898-1221(91)90145-T)
- [20] Dowson, D. (1966). Paper 12: Modes of lubrication in human joints. In *Proceedings of the Institution of Mechanical Engineers, Conference Proceedings*, pp. 45-54. https://doi.org/10.1243/PIME_CONF_1966_181_206_02

NOMENCLATURE

\bar{U}	Velocity particles of synovial fluid
R	The radius of curvature
W	Weight
N	Cohesive force of particles
C_0	Initial concentration
C_1	Final concentration
β	Porosity
H	Film thickness
S_r	Number
Sl	Stride length
R_r	Surface roughness
R_s	Surface smooth
$\bar{\mu}$	Viscosity of fluid
δ	Nature of the contacting surfaces
L_p	Length of particles